

Supplementary Information

EFFECTS OF FLOW-SELECTIVITY ON SELF-ASSEMBLY AND AUTO- ORGANIZATION PROCESSES: AN EXAMPLE

Alessandro Sorrenti,* Zoubir El-Hachemi, Joaquim Crusats and Josep M. Ribo*

Experimental Details: Synthesis and Identification Data of H₄TPPF₅S₃; Solution Preparation

5-(pentafluorophenyl)-10,15,20-triphenyl-21H,23H-porphine (H₂TPPF₅) was synthesized as previously described.^{S11} Spectroscopic data and purity as reported in the original report.

5-(pentafluorophenyl)-10,15,20-triS(4-sulfonatophenyl)-21H,23H-porphine (H₂TPPF₅S₃)

120 mg of H₂TPPF₅ were put in a round bottom flask (10 ml) and kept in an ice-bath for 10 min. Then 4 ml of sulfuric acid (at 2°C) were added and the mixture was heated to 100°C and stirred for 6 h. When the sulfuric acid was added, the mixture changed colour from purple to green. The stirring was continued for 19 h at room temperature. Then 50 ml of cold water were added and the mixture was centrifuged. The precipitate of porphyrin was separated and neutralized with a saturated solution of Na₂CO₃ to pH=7. Extractions with CH₂Cl₂, eliminated unsulfonated H₂TPPF₅. The water phase containing salt and sulphonated porphyrin was evaporated, then 150 ml MeOH were added to the residue and the mixture was heated to reflux for 30 min. The hot mixture was filtrated and the MeOH was rotary evaporated. H₂TPPF₅S₃ was purified by repetitive column chromatography in reverse phase (SiO₂-C18) using a water/methanol gradient. The purity of the porphyrin fractions was tested by HPLC on a Nucleosil 120-5C18 column, using a gradient from a mixture of methanol and tetrabutylammonium phosphate buffer (3 mmol l⁻¹; pH 7) (1:1) to pure methanol, over 30 min (t_R= 19,5 min).

Visible spectrum (H₂O), λ_{max} (ε) 412 (350000), 514 (13679), 549 (4470), 579 (5526), 631 (2210).

¹H NMR(300MHz), δ (DMSO): 9,20-9,19 (m, 2H, β-pyrrolic), 8,93-8,91 (m, 2H, β-pyrrolic), 8,88 (m, 4H, β-pyrrolic), 8,22-8,18 (m, 6H, o-Ar), 8,07-8,05 (m, 6H, m-Ar)

Solutions for the standard experiments (experiments corresponding to the Fig. 1 of the principal text). Samples for UV/Vis and RLS experiments were prepared by adding the necessary volume of a 0.3-0.5 mM porphyrin stock solution to the proper amount of Milli-Q water in a 10 ml flask, followed by the addition of the proper amount of 1M HCl (final HCl concentration 0.1 M). The final porphyrin concentration was 12 μM unless otherwise specified. The obtained solution was split into two aliquots and each of them was transferred into a 1cm quartz cuvette. One cuvette was kept under magnetic stirring (vortex stirring conditions) while the other was left quiet (stagnant conditions) or strongly shaken

The concentration of the porphyrin stock solutions was checked by UV-vis spectroscopy (ε = 350.000 mol⁻¹ L cm⁻¹ at 412 nm).

UV/Vis Spectra (evolution with time and type of stirring)

Kinetic Measurements

The evolution of the aggregation was followed by UV/Vis spectroscopy. In the experiments described in the principal text the conditions of preparation of the solution and for the starting of the aggregation were fixed to achieve a slow aggregation rate and a better reproducibility of the J-aggregate growth.

The measurements at the early stages of aggregation (1cm square section UV/Vis cuvette), once aggregation was started disturbing mechanically the metastable solution (case of stagnant conditions), were performed in a fast response J&M TIDAS spectrophotometer instrument attached to an Applied-Photophysics stopped-flow mixing unit. The aggregation for times longer than 12 hours (for example Fig. 1 in principal text) was followed in a Cary-Varian 500 Scan spectrophotometer. It is worth noting that a good distinction between the 488 nm and 492 bands is only possible at a good spectrometric resolution (Cary-Varian 500 SCAN) and the very low intensity values of the aggregates at the first stage of the aggregation require a high sensitive instrument (J&M TIDAS).

Stop-flow: Measurements in the full 800 nm – 300 nm range were performed with a J&M TIDAS spectrophotometer and specific software for the data analysis [S11]. For measurements with $t_{1/2} < 7$ s an Applied-Photophysics stopped-flow instrument connected to the above spectrometer was used. All experiments failed to start the aggregation process.

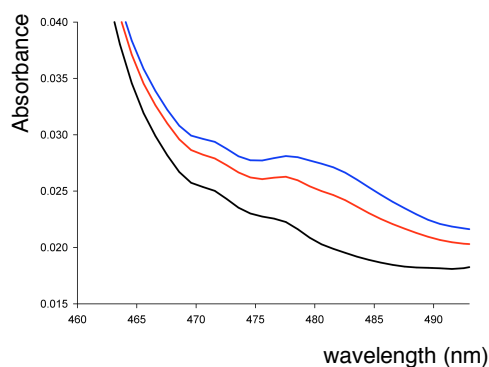


Fig. S1. For a 12 μ M porphyrin solution in stagnant conditions detection of oligomers at the first aggregation stages (5 min, 40 min and 70 min). First the trimer about 471 nm was detected together with species absorbing around 477 nm that can be attributed to the tetramer. The species at 482 (pentamer or hexamer) appears later in this specific experiment. Commonly the 477 nm species is detected only at the beginning of the aggregation and with an intensity lower than that of the 482 nm species. At longer reaction times only the oligomeric species at 470 nm and 482 nm can be detected, which later are overtaken by the final J-aggregate (488 nm).

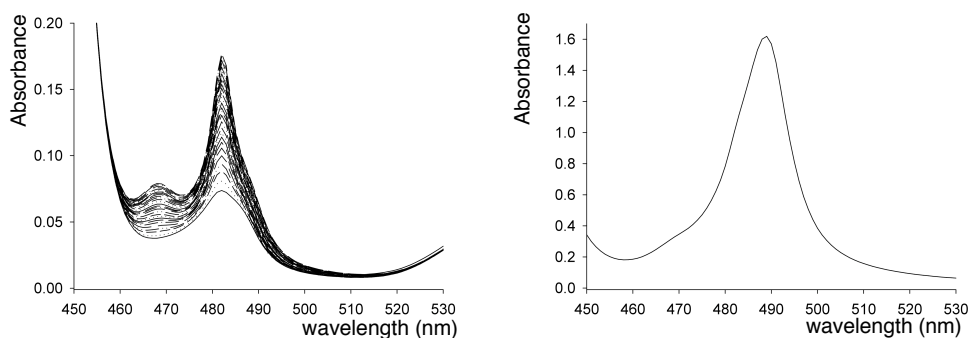


Fig. S2. Aggregation of a solution of $H_4TPPF_5S_3$ (24 μ M) in stagnant conditions. Left: spectra recording every 0.3 min for 10 min: the initial spectra at a time zero is the consequence of the primary nucleation phenomenon. Right; the same solution after 24h.

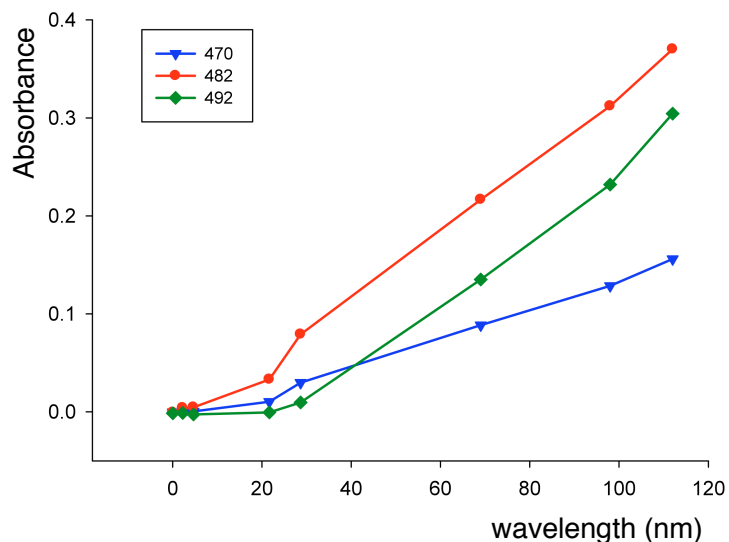


Fig. S3. Time evolution of the aggregate species under vortex stirring conditions (data from the experiment of Fig. 1 in the principal text). The three species shows an induction period followed by an exponential growth characteristic for autocatalysis. The autocatalytic growth of the 492 nm J-aggregate arises once the autocatalytic growth of the 482 nm and 470 nm species has already occurred.

RLS Spectra

Resonance light scattering measurements were performed on a PTI spectrofluorimeter in L geometry equipped with a Xe lamp (LPS 220B) and a photomultiplier detection system PTI 814, by operating in the synchronous scanning mode in which the excitation and emission monochromators were coupled to scan simultaneously.

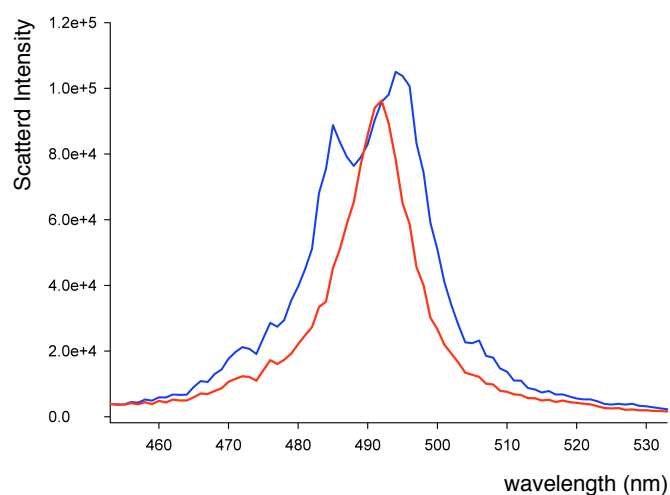


Fig. S4. RLS spectra for stagnant standard solutions 24h aged (red line; RLS band corresponding to the 488 nm species) and magnetically vortex stirred (blue line; showing the RLS bands of the 492 nm and the 482 nm species). Note that the scattering peaks are red shifted by 3 nm relative to the absorption peaks in agreement with the expected RLS peaks in respect to the absorption peaks (Miller, G. J. *Phys. Chem.* **1978**, 82, 616-618) accordingly to previous reports.

AFM Measurements

AFM images were obtained using a Multimode AFM (Veeco, Santa Barbara, CA) controlled by a Nanoscope IIIA electronics (Digital Instruments, Santa Barbara, CA) operating in tapping mode in air at room temperature (20°C) and typical relative humidity of 40%. Images were acquired in tapping mode. Drive amplitude was minimized in order to reduce the interaction between the probe and the sample. The measurements were performed at minimum Amplitude Setpoint value so as to maintain the sample integrity. Used AFM probes were silicon oxide, rectangular beam, with a nominal spring constant of 40 nN/nm (T300R-W, VistaProbes, Phoenix, AZ).

The reported images correspond to the observation of different samples deposited under the same experimental conditions and were imaged in several points of the surfaces in order to assess the homogeneity and type of the deposited particles.

Sample deposition procedure: One drop of the solution (~50 µl) was brought in contact with a freshly cleaved HOPG surface during 40 seconds. The solution was then blotted off with the tip of a filter paper and finally the HOPG surface was blow-dried with a N₂ stream.

It was necessary to perform the AFM experiments on fairly aggregated H₄TPPF₅S₃ solution *i.e.* featuring an appreciable concentration of the J-aggregates in comparison with the monomeric porphyrin (more or less the same absorbance). Otherwise, in the presence of a significant amount of monomeric diprotonated porphyrin in the solution, a homogeneous monolayer of this species, with a regular thickness of 0.8 nm, is formed (measured by section analysis along various holes, see Ref. 5b in the main text), which prevents the adhesion of the smaller J-aggregated to the HOPG surface (only some large ribbon aggregates, were observed). At this concentration conditions for the J aggregates, both the species at 488 and 492 are present in solution (the latter dominating in the vortex stirred solutions). In order to infer the thickness of the two kinds of aggregates a statistic evaluation was performed by measuring the height of a large number of particles (>100) through section analysis. Different regions of the surface for different depositions were taken into account for each sample. At least three samples of stagnant and vortex stirred solution were studied. The particle height shows a clear bimodal distribution with two peaks of different population in stagnant and vortex magnetically stirred solution.

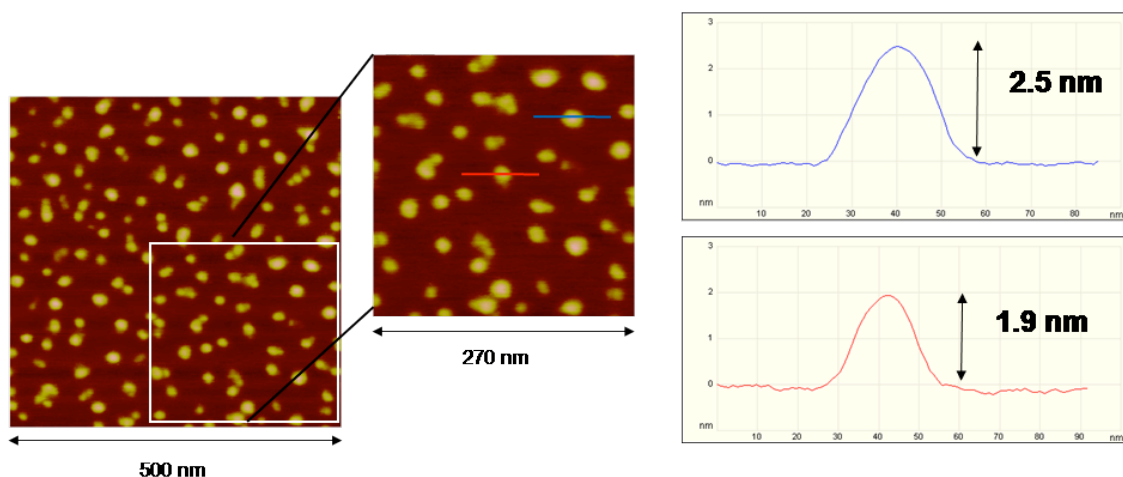


Fig. S5. AFM (tapping mode) images of an aggregate solution showing a high proportion of the first stage J-aggregates (less than three days old solution). The corresponding UV/Vis spectra showed the absorption band of the 488 nm species and a shoulder of the 492 nm. The section analysis shows the presence of two type of particles of different thickness. Several analysis of different samples showing the presence or the absence of the shoulder at 492 allows to assign associate particless with thicknes 1.90 ± 0.15 nm to the 492 nm species and particles of thickness 2.45 ± 0.20 nm to the 488 nm species

Extended Exciton Coupling Estimation of the Oligomer Chain Length

In a multiple 1d extended exciton coupling, the simple point-dipole model predicts that the interaction energy (E_n) of the splitting for a determined length n is related to the energy of the infinite extended interaction (E_∞) by the expression [SI2]

$$E_n = E_\infty \cos\left(\frac{\pi}{n+1}\right)$$

Fig. S6 shows the expected wavelength for the oligomers assuming different origin for the J-aggregate band. E_∞ corresponds to the energy difference between the monomer (433 nm) and the 488 nm J-aggregate in Fig. S6a and to that between the monomer and the 492 J-aggregate in Fig. S6b. Fig S6c and S6d correspond respectively to the case of a finite coherence length ($n = 16$; ref-[4b] in principal text) for the 488 nm and the 492 absorption (respectively Fig. S6c and Fig. S6d). Notice that the previously proposed $n = 16$ corresponds to a low value of coherence length. However, the Fig. S6 indicates that; i) the dimer absorption cannot be detected because of the strong monomer absorption at the beginning of the aggregation, ii) the absorption at 470 nm must correspond to the trimeric exciton coupling for any of the possible scenarios and iii) the absorption at 482 nm would correspond to the pentameric exciton or to the hexameric exciton coupling. Notice that the 482 nm absorption maintains a fixed wavelength during all the aggregation process, which supports the assignation of this signal to only one oligomeric species. It is worth noting that in some few experiments in stagnant conditions at the very early stages also an absorption band at 477 nm was detected (Fig. S1); the absorption of this species agree with that of the tetramer and once formed it also show autocatalysis and compete with the growth of the 482 species.

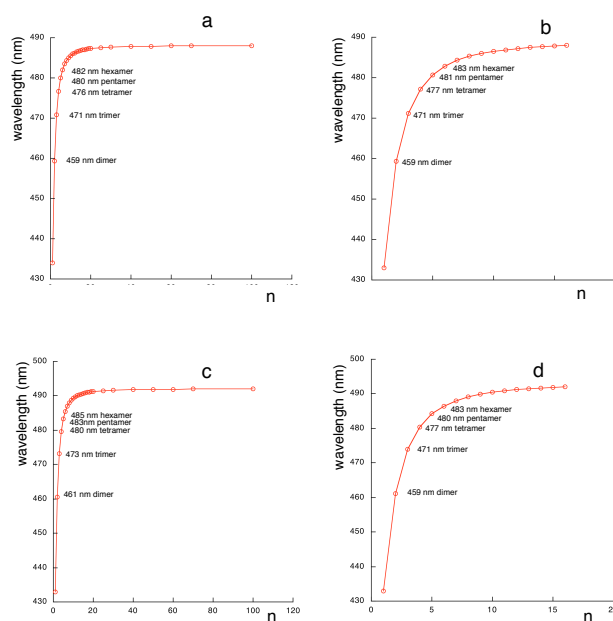


Fig. S6. Estimation of the wavelength for the extended exciton coupling [SI2] for different chain lengths. Up left 488 nm corresponds to the infinite extended coupling. Up right 488 nm corresponds to a coherence length of $n=16$. Down left 492 nm corresponds to the infinite extended coupling. Down right 492 nm corresponds to a coherence length of $n=16$. The results point that the species at 469 nm correspond to a dimer, the species at 477 nm to a tetramer and the species at 482 nm to a pentamer or more probably to a hexamer.

References Supporting Information

(SI1) Portela, C. F.; Brunckova, J.; Richards, J. L.; Schöllhorn, B.; Iamamoto, Y.; Magde, D.; Traylor, T. G.; [Sa] Binstead, R. A.; Zuberbuhler, A. D.; Jung, B. SPECTFIT32.[3.0.34]. Spectrum Software Assoc.

[SI2] a) Czikkely, V.; Forsterling, H. D.; Kuhn, H. *Chem. Phys. Lett.* **1970**, *6*, 207-210. b) Ribo J. M.; Bofill, J. M.; Crusats, J.; Rubires, R. *Chem. Eur. J.* **2001**, *7*, 2733-2737.